



Analysis of *ent*-kaurenoic acid by ultra-performance liquid chromatography-tandem mass spectrometry



Sho Miyazaki^a, Honoka Kimura^b, Masahiro Natsume^b, Tadao Asami^a, Ken-ichiro Hayashi^c, Hiroshi Kawaide^b, Masatoshi Nakajima^{a,*}

^a Department of Applied Biological Chemistry, The University of Tokyo, Tokyo 113-8657, Japan

^b Institute of Agriculture, Tokyo University of Agriculture and Technology, Tokyo 183-8509, Japan

^c Department of Biochemistry, Okayama University of Science, Okayama 700-0005, Japan

ARTICLE INFO

Article history:

Received 24 April 2015

Received in revised form

22 May 2015

Accepted 26 May 2015

Available online 30 May 2015

Keywords:

ent-Kaurenoic acid

Gibberellin

LC–MS/MS

Moss

MRM

Phytoalexin

ABSTRACT

ent-Kaurenoic acid (KA) is a key intermediate connected to a phytohormone gibberellin. To date, the general procedure for quantifying KA is by using traditional gas chromatography–mass spectrometry (GC–MS). In contrast, gibberellins, which are more hydrophilic than KA, can be easily quantified by liquid chromatography–tandem mass spectrometry (LC–MS/MS). In this study, we have established a new method to quantify KA by LC–MS/MS by taking advantage of a key feature of KA, namely the lack of fragmentation that occurs in MS/MS when electrospray ionization (ESI) is in the negative mode. Q1 and Q3 were adopted as identical channels for the multiple reaction monitoring of KA. The method was validated by comparing with the results obtained by selected ion monitoring in GC–MS. This new method could be applicable for the quantification of other hydrophobic compounds.

© 2015 The Authors. Published by Elsevier B.V. This is an open access article under the CC BY-NC-ND license (<http://creativecommons.org/licenses/by-nc-nd/4.0/>).

1. Introduction

ent-Kaurenoic acid (KA) is a key intermediate of gibberellin (GA), a diterpene phytohormone, which regulates various aspects of plant growth, such as germination, stem elongation, and flowering. As shown in Fig. 1, GA biosynthesis in flowering plants is initiated by the conversion from geranylgeranyl diphosphate (GGDP) to *ent*-kaurene by two kinds of diterpene cyclases [1,2]. *ent*-Kaurene is then converted to gibberellin A₁₂ (GA₁₂) via KA, catalyzed by two P450 enzymes, *ent*-kaurene oxidase (KO) and KA oxidase (KAO) [3,4]. Finally, GA₁₂ is converted to bioactive GA₄ by two kinds of 2-oxoglutarate-dependent dioxygenases, 20-oxidase and 3-oxidase [5,6].

In general, endogenous levels of GAs in a plant are quite low, in a range of 10^{−15}–10^{−9} g g^{−1} fresh weight. However, a few quantitative methods exist to elucidate the relationships between fluctuations in GAs and various changes in plants, such as gas or liquid chromatography combined with mass spectrometry (GC–MS or LC–MS). After

tandem mass spectrometry (MS/MS) was developed, some groups reported that GAs could also be quantified from a smaller amount of plant material and more easily pre-purified by using solid-phase extraction with LC–MS/MS [7–9]. Unlike GAs, GC–MS is now frequently used to quantify its hydrophobic intermediates such as *ent*-kaurene and KA.

In this study, we show that endogenous KA in plant material can also be quantified by LC–MS/MS with multiple reaction monitoring (MRM). Our method is expected to be a useful tool for the quantification of many hydrophobic compounds that are not easily analyzed by LC–MS/MS.

2. Materials and methods

2.1. Chemicals and reagents

Both authentic KA and deuterium-labeled KA (d₂-KA) were purchased from the laboratory of Prof. L.N. Mander (Australian National Univ., Canberra, Australia). Formic acid (FA) and methanol (MeOH) were purchased from Kanto Chemical Co. Ltd. (Tokyo, Japan).

2.2. Plant materials

Hypnum plumaeforme collected in Okayama (Japan) was used

Abbreviations: ESI, electrospray ionization; GA, gibberellin; GC, gas chromatography; KA, *ent*-kaurenoic acid; KO, *ent*-kaurene oxidase; KAO, *ent*-kaurenoic acid oxidase; LOD, limit of detection; LOQ, limit of quantitation; MRM, multiple reaction monitoring; MS/MS, tandem mass spectrometry; SIM, selected ion monitoring; LC, liquid chromatography

* Corresponding author.

E-mail address: anakajm@mail.ecc.u-tokyo.ac.jp (M. Nakajima).

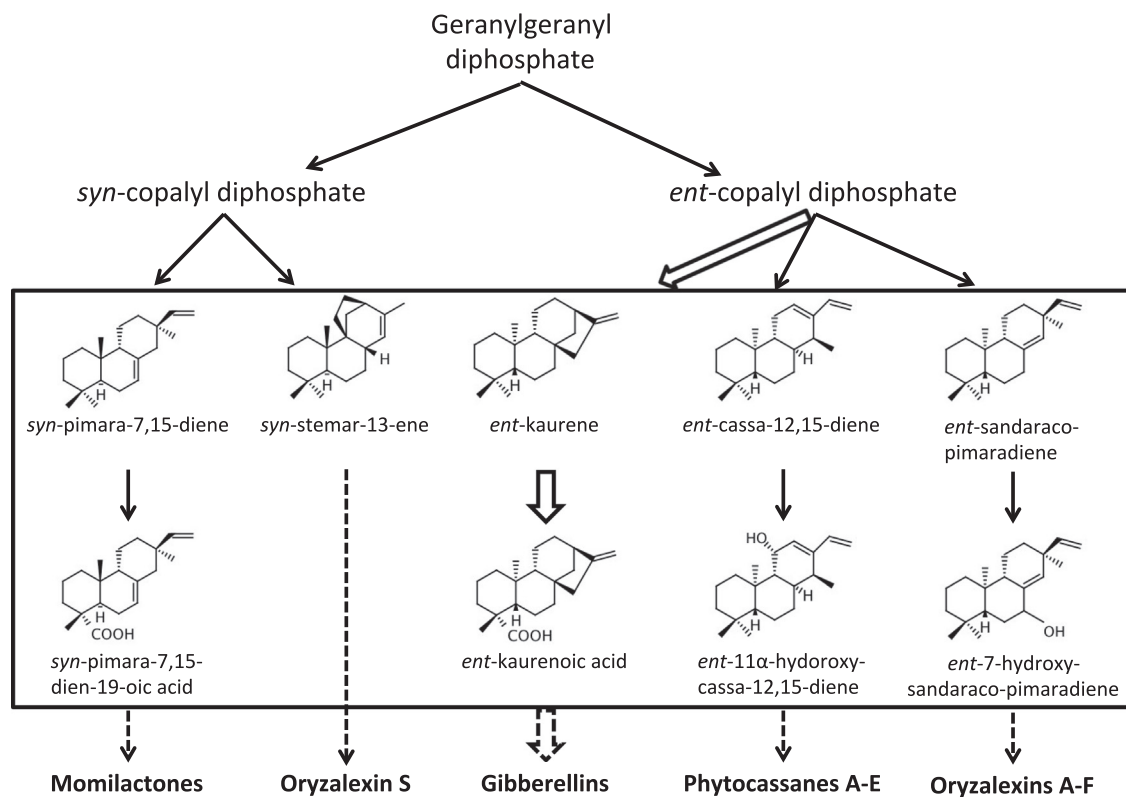


Fig. 1. Proposed biosynthetic pathway of phytoalexin in rice and GA biosynthetic pathway. The biosynthetic pathways of gibberellins (open arrows) and diterpene phytoalexins (solid arrows) are shown. Dashed arrows indicate multiple enzymatic reactions. The products of the biosyntheses, including momilactones, phytocassanes and oryzalexin S, could be analyzed by LC–MS/MS, whereas the hydrocarbon and its oxide (indicated by box) are usually analyzed by GC–MS.

[10]. The moss cultures were grown on BCD-ATG medium [1 mM MgSO₄, 1.84 mM KH₂PO₄, 10 mM KNO₃, 45 μM FeSO₄, 1 mM CaCl₂, 0.22 μM CuSO₄, 0.19 μM ZnSO₄, 10 μM H₃BO₃, 0.10 μM Na₂MoO₄, 2 μM MnCl₂, 0.23 μM CoCl₂, 0.17 μM KI, 5 mM [NH₄]₂C₄H₄O₆, 0.5% (w/w) glucose and 0.8% (w/w) agar] at 25 °C under continuous white light (60 μmol m⁻² s⁻¹). Protonemal cells were retrieved and then immediately immersed in liquid nitrogen. Samples were stored at –80 °C.

2.3. Extraction and purification of KA

Three sets of frozen plant tissues (300 mg) were homogenized five times with 1500 rpm for 30 s in 80% (v/v) MeOH containing 5% (v/v) FA as the extraction solution containing one 10 mm stainless bead using Shake Master NEO (Bio Medical Science, Tokyo, Japan). d₂-KA (10 ng) was added to the extraction solution as an internal standard. The homogenized samples were spun (200 rpm) at 4 °C overnight. The homogenates were then centrifuged (1570 × g, 5 min, 4 °C) and endogenous KA was re-extracted from the resulting pellets in the same solution twice. The combined extracts were evaporated to a water phase using a vacuum evaporator centrifuge (Iwaki Glass, Chiba, Japan) and purified using an Oasis MCX cartridge column (60 mg, 3 cc, Waters) activated with MeOH and pre-equilibrated with 5 mM FA. The evaporated samples were dissolved in 5 mM FA and loaded onto the cartridges, which were washed with 5 mM FA. Columns were then run to dryness, and KA was eluted with MeOH. Elutes were evaporated to dryness. The sample was dissolved in 25 mM NH₄HCO₃ before loading onto an Oasis MAX cartridge column (60 mg, 3 cc, Waters). The column was first activated with MeOH then equilibrated with 25 mM NH₄HCO₃ before loading the sample. Columns were then washed with MeOH and KA was eluted with 0.2 M FA in MeOH, which was evaporated to dryness.

2.4. LC–MS/MS conditions

An Acquity UPLC™ system (Waters, Milford, MA, USA), consisting of a binary solvent manager and a sample manager coupled to a Xevo TQ MS triple-stage quadrupole mass spectrometer (Waters MS Technologies, Manchester, UK), was equipped with an electrospray ionization (ESI) interface. The entire UPLC–MS system was controlled by MassLynx™ Software (version 4.1, Waters).

The dried samples were reconstituted in 100 μL of 10 mM FA in 10% (v/v) MeOH, and 10 μL of each sample was then injected onto a reversed-phase UPLC column (Acquity UPLC® BEH C18, 2.1 mm × 50 mm, 1.7 μm, Waters) with a guard column (Acquity UPLC® BEH C18 VanGuard™ Pre-column, 1.7 μm, 2.1 mm × 5 mm, Waters) coupled to the ESI–MS/MS system. KA was analyzed in the negative ion mode as [M–H][–]. KA was analyzed by a linear gradient of 1% (v/v) FA in water (A) and 1% FA in MeOH (B) at a flow rate of 0.20 mL/min, from 80:20 A:B (v/v) to 40:60 (v/v) over 2 min. Then, gradient to 100% of solvent B in 9 min. Finally, the column was washed with 100% of solvent B for 4 min and equilibrated to initial conditions. The instrument was operated as follows: capillary voltage 2.5 kV, desolvation temperature 400 °C, source temperature 150 °C, cone gas flow 50 L h⁻¹, desolvation gas flow 800 L h⁻¹.

2.5. GC–MS conditions

Full-scan GC–MS analysis of KA was performed using a mass spectrometer connected to a gas chromatograph (GCMS-QP2010 plus, Shimadzu, Kyoto, Japan). The methylated derivative of KA was reconstituted in 5 μL of MeOH, and 1 μL of each sample was injected (250 °C) into a DB-1 column (0.25 mm i.d. × 30 m, 0.25 μm film thickness; Agilent Technology, CA, USA). The column temperature was kept at 120 °C for 1 min, then increased at a rate

of $50\text{ }^{\circ}\text{C min}^{-1}$ to $200\text{ }^{\circ}\text{C}$, and then increased at a rate of $20\text{ }^{\circ}\text{C min}^{-1}$ to $280\text{ }^{\circ}\text{C}$. The flow rate of the carrier He gas was 1.22 ml min^{-1} , and mass spectra were acquired by scanning from m/z 50 to 400.

3. Results and discussion

3.1. Detection of KA by LC–MS/MS

There are a few reports on the detection of KA by LC–MS or LC–MS/MS [11,12], but no reports have quantified KA with the MRM method. At first, we observed the fragmentation of authentic KA

with a single scan mode of LC–MS/MS (ionization, ESI; negative mode). As a result, LC–MS provided a profile in which no fragmented ions were detected except for the parental ion of KA at m/z 301 ($[\text{M}-\text{H}]^{-}$, $t_{\text{R}}=8.94\text{ min}$, Fig. 2A and B). Secondly, to apply the MS/MS function, we set selected ion monitoring (SIM) at m/z 301.3 on Q1, and then scanned its daughter ions on Q3 after charging some energy on Q2 for the collision of the selected ion at m/z 301.3. The KA was detected similar to that shown in LC–MS, in a range of 0–40 eV charged on Q2 (Fig. S1A). Surprisingly, no fragmentation of the selected ion was detected (data not shown). These observations probably indicate that the lack of KA fragmentation might be a unique characteristic that could be applied for the detection of KA using LC–MS/MS. To examine this

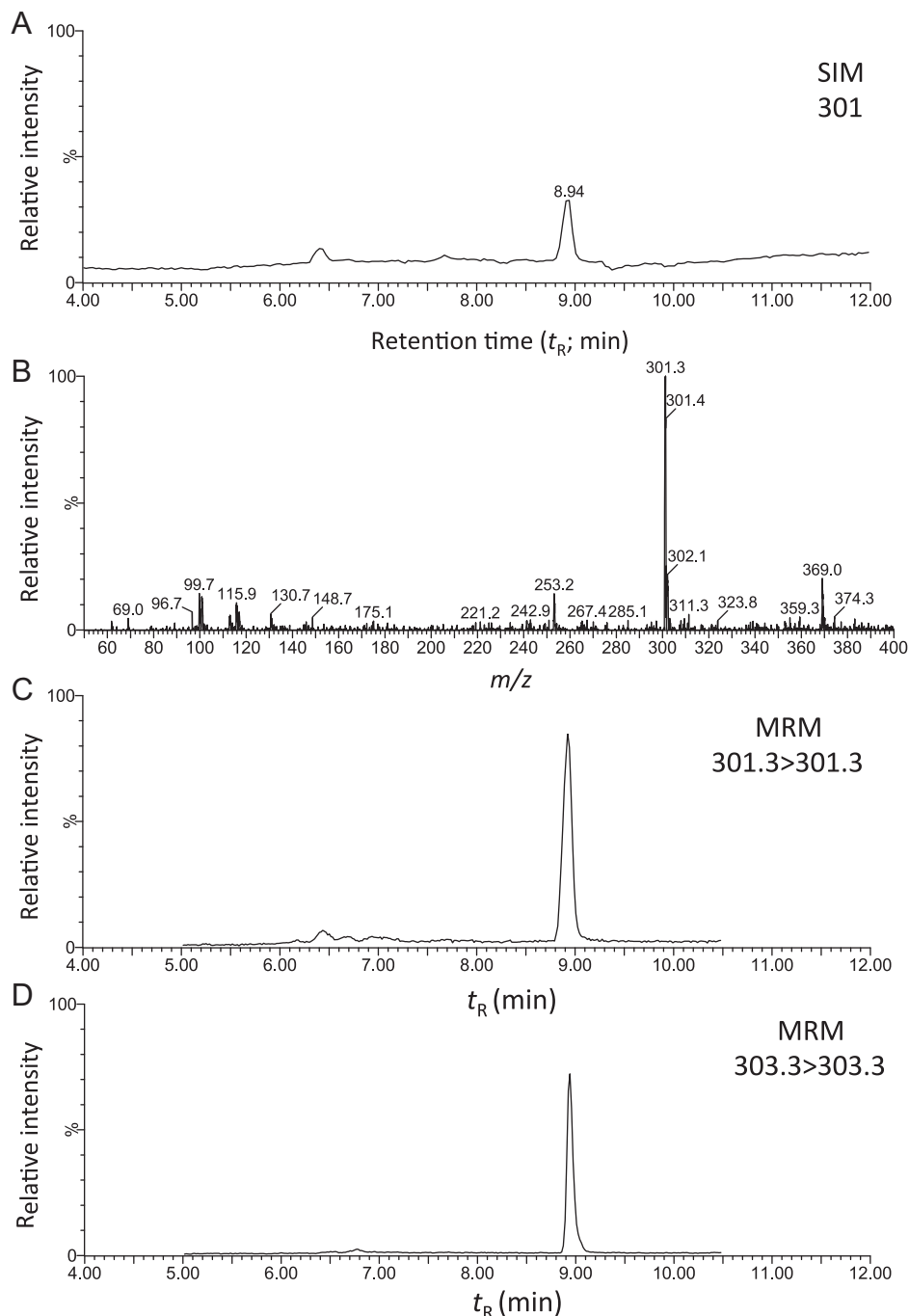


Fig. 2. LC–ESI–MS/MS spectra of *ent*-kaurenoic acid Chromatogram of $[\text{M}-\text{H}]^{-}$ ion at m/z 301 using negative SIM mode (A) and ESI–MS spectra using 54 eV cone voltage (B). Chromatogram using negative MRM mode for KA ($301.3 > 301.3$) (C) and d2-KA ($303.3 > 303.3$) (D). Intensity of (A), (C) and (D) are 1.50×10^5 as 100%.

possibility, we set the tandem SIMs at m/z 301.3 ($301.3 > 301.3$) on both Q1 and Q3. With this unusual MRM condition, it was expected that only unfragmented ions derived from KA should be detected on Q3 and that ions from other molecules would not be detected because of their fragmentation on Q2. As shown in Fig. S1B, the daughter ion of KA at m/z 301.3 was still detected after charging its collision energy in a range of 0–20 eV on Q2. Finally, it

was elucidated that the daughter ion of KA could be detected most efficiently after charging with 6.0 eV of collision energy (Fig. S1B).

We also optimized the cone voltage on Q1: the SIM at m/z 301.3 on Q1, after charging cone voltage by 54 eV, showed the highest sensitivity for the detection of KA, in the range of 0–70 eV (Fig. S2). Hence, we established the so-called “pseudo MRM” condition for the detection of KA with an LC–MS/MS (Fig. 2C). To confirm this MRM method, we applied tandem SIMs at m/z 303.3 on both Q1 and Q3 to detect d_2 -KA, which was successfully detected by LC–MS/MS (Fig. 2D).

3.2. Validation of the method for KA quantification

To validate this newly developed method, various concentrations of authentic KA solution were prepared. The detection of these concentrations of KA was compared by two analytical procedures: GC–MS and LC–MS/MS. To detect KA with GC–MS, we derivatized KA to its methyl ester just prior to its injection into the GC column. Fig. 3 shows calibration curves of KA; for the GC–MS analysis, the curve became linear in the range of 800–13,000 ng ml⁻¹. On the other hand, it became linear in the range of 0.8–13 ng ml⁻¹ for the LC–MS/MS analysis. The precision of both methods was determined as 7.20 for GC–MS and 2.87 for LC–MS/MS by calculating relative SD values for each spiking level. In addition, the accuracy of both methods was also assessed as 7.65 for GC–MS and 2.69 for LC–MS/MS on a percentage basis (Table S1). The limits of detection (LOD) and quantitation (LOQ) were evaluated by using $3 \times s_{y/x}/a$ and $10 \times s_{y/x}/a$, respectively [13] where the $s_{y/x}$ value indicates the SD value of the calibration curve and a indicates the slope of the regression curve. The LOD and LOQ for GC–MS were 1400 ng ml⁻¹ and 4400 ng ml⁻¹, respectively and those for LC–MS/MS were 0.59 ng ml⁻¹ and 1.8 ng ml⁻¹, respectively (Table S1). Based on these values, the method employing LC–MS/MS was evaluated as being ca. 2000 times more sensitive than the traditional GC–MS method.

To confirm the analytical accuracy of LC–MS/MS, the quantificational data obtained was compared directly with data obtained from GC–MS by spiking a mixture of KA (800 ng ml⁻¹) and d_2 -KA (400 ng ml⁻¹). The methylated derivatives of KA and d_2 -KA were analyzed by GC–MS and the same compounds diluted 2000-fold

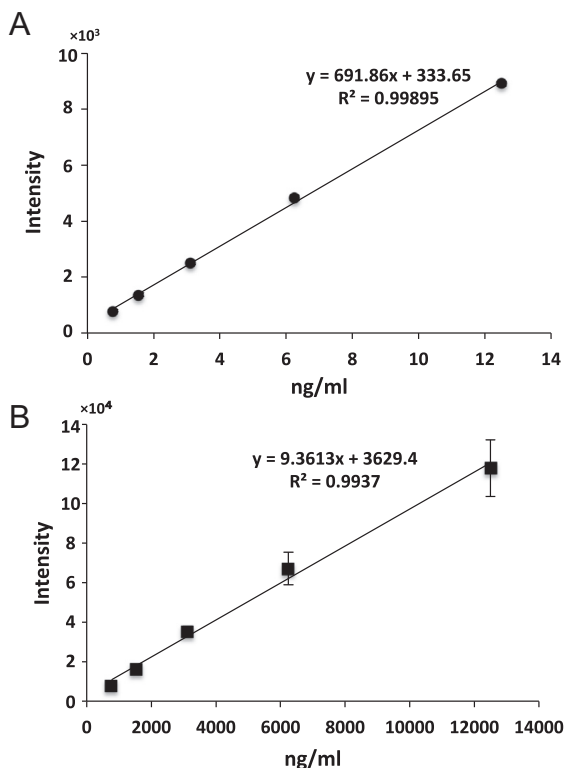


Fig. 3. Calibration curves of KA by using LC–MS/MS (A) and GC–MS (B) error bars indicate standard deviation. Y indicates the peak area of the ion intensity of the MRM mode ($301.3 > 301.3$) for LC–MS and the SIM mode ($m/z=316$) of KA for GC–MS. X is ng/ml. $n=5$.

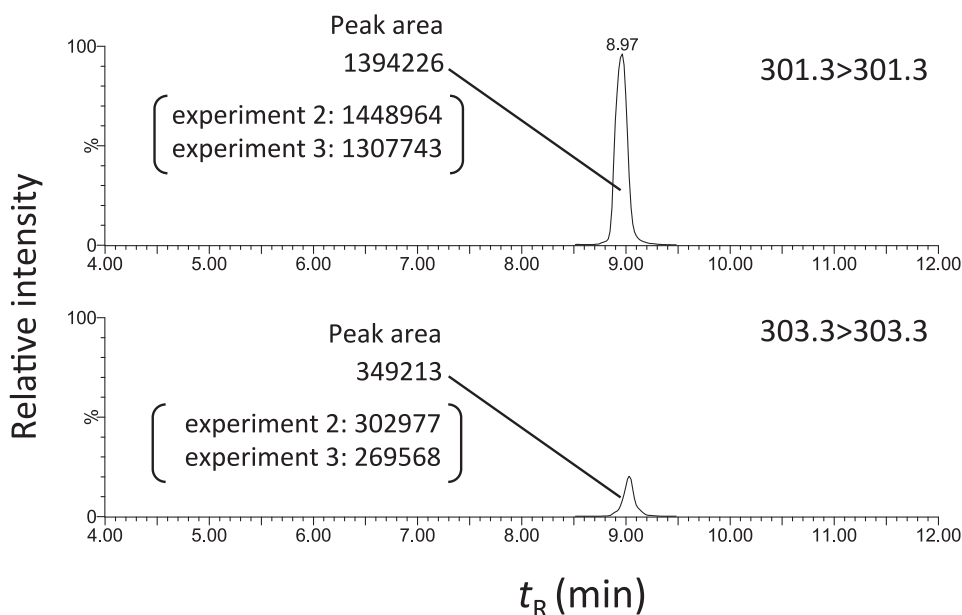


Fig. 4. Extraction and purification of *ent*-kaurenoic acid in moss. LC chromatogram of MRM mode ($301.3 > 301.3$ for *ent*-kaurenoic acid, $303.3 > 303.3$ for d_2 -*ent*-kaurenoic acid) using 54 eV of cone voltage and 6 eV of collision voltage (A). Intensity is 1.00 e⁷ as 100%. The peak area of the ion intensity of the MRM mode ($301.3 > 301.3$) and ($303.3 > 303.3$) were indicated from independent experiments. $n=3$.

were analyzed by LC–MS/MS. Analytical recovery (measured value/true amount) of LC–MS/MS and GC–MS was 99.8% and 98.5% of the true amount, respectively (Table S1).

3.3. Quantification of KA in a moss

A moss *H. plumaeforme* has a high amount of *ent*-kaurene, a direct precursor of KA (unpublished data). We applied our developed method to quantify endogenous KA in this moss after extraction and semi-purification with two solid-phase cartridge columns as described in Section 2. As an internal KA standard, 10 ng of d_2 -KA was used in each analysis. As shown in Fig. 4, no interfering substances such as chlorophyll or other natural pigments were observed in both the MRM transitions for KA (301.3 > 301.3) or for d_2 -KA (303.3 > 303.3). As a result, the endogenous KA in *H. plumaeforme* was shown to be 75.7 ng g⁻¹ FW with LC–MS/MS.

3.4. Closing remarks

In this study, we showed that endogenous KA in plant materials could be quantified by using LC–MS/MS. This method is unique in that identical SIMs are set for both Q1 and Q3. To develop this method, we took advantage of a key characteristic of KA: the parental ion is not easy to fragment even after charging collision energy on Q2. This method may be applicable for substances with a similar characteristic as KA such as many diterpenes oxidized from a hydrocarbon, as shown in Fig. 1 [10,14–18].

Acknowledgments

This work was supported by Japan Society for the Promotion of Science (JSPS) KAKENHI Grant Number (23113005, 24380060 and 15H04492).

Appendix A. Supplementary material

Supplementary data associated with this article can be found in the online version at <http://dx.doi.org/10.1016/j.bbrep.2015.05.010>.

References

- [1] T.P. Sun, Y. Kamiya, The *Arabidopsis* GA1 locus encodes the cyclase *ent*-kaurene synthetase A of gibberellin biosynthesis, *Plant Cell* 6 (1994) 1509–1518.
- [2] S. Yamaguchi, T.P. Sun, H. Kawaide, Y. Kamiya, The GA2 locus of *Arabidopsis*

- thaliana* encodes *ent*-kaurene synthase of gibberellin biosynthesis, *Plant Physiol.* 116 (1998) 1271–1278.
- [3] C.A. Helliwell, A. Poole, W.J. Peacock, E.S. Dennis, *Arabidopsis ent* -kaurene oxidase catalyzes three steps of gibberellin biosynthesis, *Plant Physiol.* 119 (1999) 507–510.
- [4] C.A. Helliwell, P.M. Chandler, A. Poole, E.S. Dennis, W.J. Peacock, The CYP88A cytochrome P450, *ent*-kaurenoic acid oxidase, catalyzes three steps of the gibberellin biosynthesis pathway, *Proc. Natl. Acad. Sci. USA* 98 (2001) 2065–2070.
- [5] A.L. Phillips, D.A. Ward, S. Uknes, N.E. Appleford, T. Lang, A.K. Huttly, P. Gaskin, J.E. Graebe, P. Hedden, Isolation and expression of three gibberellin 20-oxidase cDNA clones from *Arabidopsis*, *Plant Physiol.* 108 (1995) 1049–1057.
- [6] J. Williams, A.L. Phillips, P. Gaskin, P. Hedden, Function and substrate specificity of the gibberellin 3 β -hydroxylase encoded by the *Arabidopsis* GA4 gene, *Plant Physiol.* 117 (1998) 559–563.
- [7] M. Kojima, T. Kamada-Nobusada, H. Komatsu, K. Takei, T. Kuroha, M. Mizutani, M. Ashkari, M. Ueguchi-Tanaka, M. Matsuoka, K. Suzuki, H. Sakakibara, Highly sensitive and high-throughput analysis of plant hormones using MS-probe modification and liquid chromatography-tandem mass spectrometry: an application for hormone profiling in *Oryza sativa*, *Plant Cell Physiol.* 50 (2009) 1201–1214.
- [8] M. Müller, S. Munné-Bosch, Rapid and sensitive hormonal profiling of complex plant samples by liquid chromatography coupled to electrospray ionization tandem mass spectrometry, *Plant Methods* 7 (2011) 37.
- [9] T. Urbanová, D. Tarkovská, O. Novák, P. Hedden, M. Strnad, Analysis of gibberellins as free acids by ultra-performance liquid chromatography-tandem mass spectrometry, *Talanta* 112 (2013) 85–94.
- [10] H. Nozaki, K. Hayashi, N. Nishimura, H. Kawaide, A. Matsuo, D. Takaoka Momi-lactone, A and B as allelochemicals from moss *Hypnum plumaeforme*: first occurrence in bryophytes, *Biosci. Biotechnol. Biochem.* 71 (2007) 3127–3130.
- [11] J.C. Gasparetto, T.M. Francisco, F.R. Campos, R. Pontarolo, Development and validation of two methods based on high-performance liquid chromatography-tandem mass spectrometry for determining 1,2-benzopyrone, dihydrocoumarin, *o*-coumaric acid, syringaldehyde and kaurenoic acid in guaco extracts and pharmaceutical preparations, *J. Sep. Sci.* 34 (2011) 740–748.
- [12] A.R.M. Costa, L.A.P. Freitas, J. Mendiola, E. Ibáñez, *Copaifera langsdorffii* supercritical fluid extraction: chemical and functional characterization by LC/MS and *in vitro* assays, *J. Supercrit. Fluids* 100 (2015) 86–96.
- [13] P. Araujo, Key aspects of analytical method validation and linearity evaluation, *J. Chromatogr. B* 877 (2009) 2224–2234.
- [14] K. Hayashi, H. Kawaide, M. Notomi, Y. Sakigi, A. Matsuo, H. Nozaki, Identification and functional analysis of bifunctional *ent*-kaurene synthase from the moss *Physcomitrella patens*, *FEBS Lett.* 580 (2006) 6175–6181.
- [15] T. Toyomasu, T. Kagahara, K. Okada, J. Koga, M. Hasegawa, W. Mitsuhashi, T. Sassa, H. Yamane, Diterpene phytoalexins are biosynthesized in and exuded from roots of rice seedlings, *Biosci. Biotechnol. Biochem.* 72 (2008) 562–567.
- [16] B. Hamberger, T. Ohnishi, B. Hamberger, A. Séguin, J. Bohlmann, Evolution of diterpene metabolism: Sitka spruce CYP720B4 catalyzes multiple oxidations in resin acid biosynthesis of conifer defense against insects, *Plant Physiol.* 157 (2011) 1677–1695.
- [17] Q. Wang, M.L. Hillwig, K. Okada, K. Yamazaki, Y. Wu, S. Swaminathan, H. Yamane, R.J. Peters, Characterization of CYP76M5-8 indicates metabolic plasticity within a plant biosynthetic gene cluster, *J. Biol. Chem.* 287 (2012) 6159–6168.
- [18] T. Toyomasu, M. Usui, C. Sugawara, K. Otomo, Y. Hirose, A. Miyao, H. Hirochika, K. Okada, T. Shimizu, J. Koga, M. Hasegawa, M. Chuba, Y. Kawana, M. Kuroda, E. Minami, W. Mitsuhashi, H. Yamane, Reverse-genetic approach to verify physiological roles of rice phytoalexins: characterization of a knockdown mutant of OsCPS4 phytoalexin biosynthetic gene in rice, *Physiol. Plant.* 150 (2014) 55–62.